

# Detecting dilute axion stars constrained by fast radio bursts in the Solar System via stimulated decay

Haoran Di,<sup>1,\*</sup> Zhu Yi,<sup>2,3</sup> Haihao Shi,<sup>4,5</sup> and Yungui Gong<sup>6,†</sup>

<sup>1</sup>*School of Science, East China University of Technology, Nanchang 330013, China*

<sup>2</sup>*Faculty of Arts and Sciences, Beijing Normal University, Zhuhai 519087, China*

<sup>3</sup>*Advanced Institute of Natural Sciences, Beijing Normal University, Zhuhai 519087, China*

<sup>4</sup>*Xinjiang Astronomical Observatory, CAS, Urumqi 830011, China*

<sup>5</sup>*College of Astronomy and Space Science, University of Chinese Academy of Sciences, Beijing 101408, China*

<sup>6</sup>*Institute of Fundamental Physics and Quantum Technology, Department of Physics, School of Physical Science and Technology, Ningbo University, Ningbo 315211, China*

Fast radio bursts (FRBs) can be explained by collapsing axion stars, imposing constraints on the axion parameter space and providing valuable guidance for experimental axion searches. In the traditional post-inflationary model, axion stars could constitute up to 75% of the dark matter component, suggesting that some axion stars may exist within the Solar System. Photons with energy half the axion mass can stimulate axion decay. Thus, directing a powerful radio beam at an axion star could trigger its stimulated decay, producing a detectable echo. Using this method, we find it is possible to test the existence of dilute axion stars with maximum masses ranging from  $6.21 \times 10^{-12} M_\odot$  to  $2.61 \times 10^{-10} M_\odot$ , as constrained by FRBs, within the Solar System. The resulting echo from axion stars constrained by FRBs could be detectable by terrestrial telescopes. Detecting such an echo would confirm the existence of axion stars, unravel the mystery of dark matter, and provide key evidence that some FRBs originate from collapsing axion stars. Furthermore, FRBs produced by axion star collapses could serve as standard candles, aiding in the resolution of the Hubble tension. If no echo is detected using this method, it would place constraints on the abundance of dark matter in the form of dilute axion stars with maximum masses in the range of  $6.21 \times 10^{-12} M_\odot$  to  $2.61 \times 10^{-10} M_\odot$ .

## I. INTRODUCTION

Growing evidence from various observations and theoretical frameworks has established that dark matter constitutes a substantial portion of the Universe’s energy density. Nonetheless, its exact nature remains elusive. The QCD axion [1, 2], arising from the Peccei-Quinn mechanism [3, 4] developed to resolve the strong- $CP$  problem, is a well-motivated candidate for dark matter. Additionally, string theory predicts a spectrum of axion-like particles (ALPs) across a wide mass range, a concept often referred to as the “axiverse” [5]. In this article, we use the term “axions” to encompass both QCD axions and ALPs. Axions can be produced through several mechanisms, such as the misalignment mechanism [6–9], thermal production [10, 11], the decay of string [12, 13], and primordial black hole (PBH) evaporation [14–16]. Because axions are bosons, they can attain very high phase space densities, which may result in Bose-Einstein condensation (BEC) [17] and the formation of gravitationally bound objects known as axion stars [18–22].

The unusual orbits of trans-Neptunian objects (TNOs) [23–25] and the gravitational anomalies detected by the Optical Gravitational Lensing Experiment (OGLE) [26] remain unexplained. One potential explanation is the existence of PBHs [27] or axion stars [28] with masses in the

range of  $M \sim 0.5 - 20 M_\oplus$ , which could account for the OGLE observations. To address the TNO orbital anomalies, the planet 9 hypothesis proposes an object with a mass of  $5 - 15 M_\oplus$  (approximately  $1.5 - 4.5 \times 10^{-5} M_\odot$ ) located 300 – 1000 AU from the Sun [29]. This hypothetical planet 9 could be explained as a dilute axion star [30] that was captured by the Solar System. Additionally, collapsing axion stars with specific parameters may emit millisecond-long radio bursts with peak luminosities of approximately  $10^{42}$  erg/s, which are consistent with the characteristics of observed non-repeating fast radio bursts (FRBs) [31]. These collapsing axion stars could serve as novel standard candles [32] for constraining the Hubble constant,  $H_0$ , due to their strong, intrinsic luminosity being fixed and dependent solely on the axion mass and decay constant. Other studies have also investigated the relationship between axion stars and FRBs [33–36]. If some FRBs are indeed produced by collapsing axion stars, this would impose constraints on the axion parameter space [32], providing valuable guidance for experimental searches for axions. Thus, exploring the axion parameter space in relation to FRBs is crucial, as it offers insight into the origin of FRBs and the nature of dark matter.

Photons with energy half the axion mass can trigger the stimulated decay [31, 37–40] of axions, producing an echo. This phenomenon offers a novel opportunity to search for axion dark matter. By emitting a radio beam with high power into space and detecting the resulting echo, axion dark matter may be identified and studied [41–45]. In our previous work [46], we proposed that the

\* Corresponding author: [hrdi@ecut.edu.cn](mailto:hrdi@ecut.edu.cn)

† Corresponding author: [gongyungui@nbu.edu.cn](mailto:gongyungui@nbu.edu.cn)

stimulated decay of a dilute axion star associated with planet 9 could be triggered by directing a powerful radio beam at the star, resulting in an echo could be detected by current radio telescopes. Such an observation would distinguish an axion star from a PBH [47] or other planet 9 candidates. This method offers a promising avenue for exploring the axion parameter space constrained by FRBs.

This article is organized as follows. In Sec. II, we briefly introduce the concept of dilute axion stars. In Sec. III, we review the constraints on the axion parameter space imposed by FRBs. Section IV discusses the abundance of dilute axion stars in the Universe. In Sec. V, we analyze the potential for detecting echoes from dilute axion stars, as constrained by FRBs, within the Solar System by emitting powerful radio beams into these stars. Finally, Sec. VI presents our conclusions. In this article, we adopt natural units, setting  $c = \hbar = 1$ .

## II. DILUTE AXION STARS

The QCD axion is a hypothetical pseudo-Nambu-Goldstone boson with spin-0, characterized by a small mass  $m_\phi$ , weak self-interactions, and extremely weak couplings to Standard Model particles. The invariance of the axion Lagrangian under the shift symmetry  $\phi(x) \rightarrow \phi(x) + 2\pi f_a$  requires the axion potential  $V(\phi)$  to be periodic, such that  $V(\phi) = V(\phi + 2\pi f_a)$ , where  $f_a$  represents the  $U(1)$  symmetry breaking scale, also known as the axion decay constant. Performing a series expansion of the axion potential around  $\phi = 0$ , and considering only the first two leading terms, the potential can be expressed as

$$V(\phi) = \frac{1}{2}m_\phi^2\phi^2 + \frac{\lambda}{4!}\phi^4 + \mathcal{O}\left(\frac{\lambda^2\phi^6}{6!m_\phi^2}\right), \quad (1)$$

where  $\lambda = -\kappa m_\phi^2/f_a^2$  is the coupling constant representing the attractive self-interaction of axions. The value of  $\kappa$  depends on the choice of axion potential. For the instanton potential,  $V(\phi) = (m_\phi f_a)^2 [1 - \cos(\phi/f_a)]$ , commonly used in axion phenomenology,  $\kappa = 1$ . For the chiral potential [48, 49],  $\kappa \simeq 0.34$  [49, 50]. Considering the interaction between axions and photons, the general Lagrangian for the axion is given by

$$\begin{aligned} \mathcal{L} = & \frac{1}{2}\partial_\mu\phi\partial^\mu\phi - \frac{1}{2}m_\phi^2\phi^2 - \frac{\lambda}{4!}\phi^4 - \mathcal{O}\left(\frac{\lambda^2\phi^6}{6!m_\phi^2}\right) \\ & + \frac{\alpha K}{8\pi f_a}\phi F_{\mu\nu}\tilde{F}^{\mu\nu} - \frac{1}{4}F_{\mu\nu}F^{\mu\nu}, \end{aligned} \quad (2)$$

where  $\alpha$  is the fine-structure constant representing the electromagnetic field coupling strength,  $K$  is a dimensionless quantity of order one that depends on the axion model, and  $F_{\mu\nu}$  and  $\tilde{F}^{\mu\nu}$  represent the electromagnetic field tensor and its dual, respectively. Due to their coupling with electromagnetic fields, axions can spontaneously decay into photons. This interaction has signif-

icant astrophysical implications and provides an experimental avenue for searching for these elusive particles. The spontaneous decay rate of an axion at rest into two photons is given by

$$\begin{aligned} \Gamma_\phi &= \frac{\alpha^2 K^2 m_\phi^3}{256\pi^3 f_a^2} \\ &= 1.02 \times 10^{-50} \text{ s}^{-1} K^2 \left(\frac{m_\phi}{10^{-5} \text{ eV}}\right)^3 \left(\frac{f_a}{10^{12} \text{ GeV}}\right)^{-2}. \end{aligned} \quad (3)$$

The extremely low decay rate makes it challenging to detect axions through photon signals from their spontaneous decay. For QCD axions, there exists a well-known relationship between the decay constant  $f_a$  and the axion mass [1]:

$$\begin{aligned} m_\phi &= \frac{\sqrt{m_u m_d} f_\pi m_\pi}{m_u + m_d f_a} \\ &\simeq 6 \times 10^{-6} \text{ eV} \left(\frac{f_a}{10^{12} \text{ GeV}}\right)^{-1}, \end{aligned} \quad (4)$$

where  $m_u \simeq 2.2 \text{ MeV}$ ,  $m_d \simeq 4.7 \text{ MeV}$ , and  $m_\pi \simeq 135 \text{ MeV}$  are the masses of the up quark, down quark, and pion, respectively, while  $f_\pi \simeq 92 \text{ MeV}$  is the pion decay constant. This relationship is illustrated in Fig. 1. As bosons, axions can achieve exceptionally high phase space densities, potentially leading to the formation of BECs [17] and the creation of axion stars, which are divided into dilute and dense branches [51–54]. Dilute axion stars are stable against perturbations, while dense axion stars may have lifetimes much shorter than any cosmological timescale [18, 55–58].

For a stable dilute axion star, equilibrium is maintained by the balance between attractive self-gravity and self-interactions, and the repulsive pressure from the Heisenberg uncertainty principle. This equilibrium persists as long as the star's density remains low, minimizing the influence of self-interactions. However, once the star's mass exceeds a critical threshold, determined by the strength of the attractive self-interaction coupling constant, the equilibrium is disrupted. The maximum mass  $M_{\text{max}}$  and corresponding minimum radius  $R_{\text{min}}$  of a stable axion star are given by [59, 60]

$$M_{\text{max}} \sim 5.073 \frac{M_{\text{pl}}}{\sqrt{|\lambda|}}, \quad R_{\text{min}} \sim \sqrt{|\lambda|} \frac{M_{\text{pl}}}{m_\phi} \lambda_c, \quad (5)$$

where  $\lambda_c$  is the Compton wavelength of the axion and  $M_{\text{pl}}$  is the Planck mass. When the mass of an axion star exceeds the critical mass given by Eq. (5), either due to merger events [61–67] or through the accretion of axions from the surrounding environment [68–70], self-interactions become significant, potentially leading to the collapse of the star [71–74]. Substituting the attractive coupling constant of self-interaction,  $\lambda = -\kappa m_\phi^2/f_a^2$ , and the axion's Compton wavelength,  $\lambda_c = 2\pi/m_\phi$ , into Eq. (5), the critical mass and minimum radius are ex-

pressed as

$$M_{\max} \sim 5.97 \times 10^{-12} M_{\odot} \kappa^{-1/2} \times \left( \frac{m_{\phi}}{10^{-5} \text{ eV}} \right)^{-1} \left( \frac{f_a}{10^{12} \text{ GeV}} \right), \quad (6)$$

$$R_{\min} \sim 2.41 \times 10^2 \text{ km } \kappa^{1/2} \times \left( \frac{m_{\phi}}{10^{-5} \text{ eV}} \right)^{-1} \left( \frac{f_a}{10^{12} \text{ GeV}} \right)^{-1}. \quad (7)$$

These quantities depend not only on the mass and decay constant of the axion but also on the choice of axion potential. For a general dilute axion star, we denote its mass as  $M_{\text{AS}}$  and its radius as  $R_{\text{AS}}$ .

### III. CONSTRAINTS BY FAST RADIO BURSTS

Despite the extremely low spontaneous decay rate, axion decay rates can be enhanced in the presence of ambient photons, as photons with energy equivalent to half of the axion mass can stimulate decays of axions into two photons. The change in photon number density  $n_{\lambda'}$  within a dilute axion star, resulting from axion decay and inverse decay, is governed by the Boltzmann equation [37]:

$$\begin{aligned} \frac{dn_{\lambda'}}{dt} = & \int dX_{\text{LIPS}} |\mathcal{M}(\phi \rightarrow \gamma(\lambda')\gamma(\lambda'))|^2 \\ & \times \{f_{\phi}(\mathbf{p})[1 + f_{\lambda'}(\mathbf{k}_1)][1 + f_{\lambda'}(\mathbf{k}_2)] \\ & - f_{\lambda'}(\mathbf{k}_1)f_{\lambda'}(\mathbf{k}_2)[1 + f_{\phi}(\mathbf{p})]\}, \end{aligned} \quad (8)$$

where  $\mathcal{M}(\phi \rightarrow \gamma(\lambda')\gamma(\lambda'))$  refers to the matrix element corresponding to the coupling term between axions and photons,  $f_{\phi}$  is the phase space density of axions, and  $f_{\lambda'}$  is the phase space density of photons with helicity  $\lambda'$ . After performing the phase space integration for the above equation and considering the two possible helicities of photons, the time evolution of the total photon number density becomes [37, 38]

$$\frac{dn_{\gamma}}{dt} = 2\Gamma_{\phi}n_{\phi} + \frac{16\pi^2}{m_{\phi}^3 v} \Gamma_{\phi}n_{\phi}n_{\gamma} - \frac{16\pi^2}{3m_{\phi}^3} \left( v + \frac{3}{2} \right) \Gamma_{\phi}n_{\gamma}^2, \quad (9)$$

where  $v$  is the maximum velocity of an axion within the axion star, which is roughly  $1/(2R_{\text{AS}}m_{\phi})$  as estimated using the uncertainty principle.

In Eq. (9), the first term represents spontaneous axion decay, while the second term accounts for the stimulated decay of axions in the presence of ambient photons. The third term corresponds to the inverse decay process, in which photons are converted back into axions. The component with a factor of  $3/2$  corresponds to the generation of “sterile” axions with high velocity that escape from the axion star [37]. Additionally, photons produced through spontaneous axion decay and stimulated decay

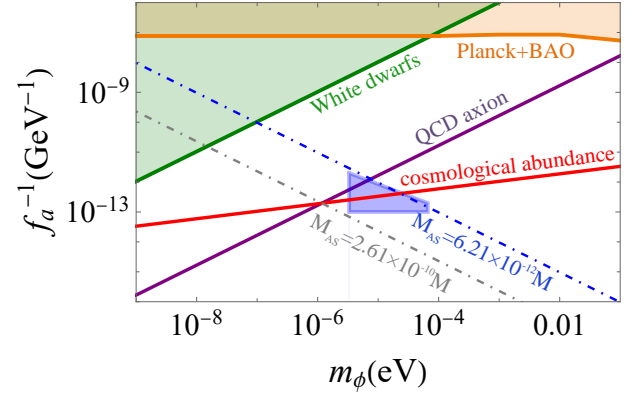


FIG. 1. Constraints on the axion parameter space. The region above the orange line is excluded based on Planck 2018 and BAO measurements [75]. A recent study [76] places a model-independent bound on QCD axions from supernova 1987A, which is stronger than the bounds from Planck and BAO. Constraints from white dwarf observations are represented by the green region [77], with recent updates provided in Ref. [78]. The purple line indicates constraints for QCD axions, while the blue region corresponds to the parameter space constrained by FRBs, where the maximum mass of dilute axion stars ranges from  $6.21 \times 10^{-12} M_{\odot}$  to  $2.61 \times 10^{-10} M_{\odot}$ .

in the presence of ambient photons can also escape from the axion star, with an escape rate of  $\Gamma_e = 1/R_{\text{AS}}$ . Integrating Eq. (9) and considering the photons that escape from the axion star, the coupled differential equations describing the evolution of the number of axions and photons within the axion star are given by [32]

$$\begin{aligned} \frac{dN_{\gamma}}{dt} = & 2\Gamma_{\phi}N_{\phi} + \frac{12\pi}{m_{\phi}^3 v R_{\text{AS}}^3} \Gamma_{\phi}N_{\phi}N_{\gamma} \\ & - \frac{2\pi(2v+3)}{m_{\phi}^3 R_{\text{AS}}^3} \Gamma_{\phi}N_{\gamma}^2 - \Gamma_e N_{\gamma}, \end{aligned} \quad (10)$$

$$\begin{aligned} \frac{dN_{\phi}}{dt} = & -\Gamma_{\phi}N_{\phi} - \frac{6\pi}{m_{\phi}^3 v R_{\text{AS}}^3} \Gamma_{\phi}N_{\phi}N_{\gamma} \\ & + \frac{4\pi v}{m_{\phi}^3 R_{\text{AS}}^3} \Gamma_{\phi}N_{\gamma}^2. \end{aligned} \quad (11)$$

However, even for dilute axion stars in a critical state, the photon number  $N_{\gamma} \simeq (2\Gamma_{\phi}/\Gamma_e)N_{\phi}$  resulting from spontaneous decay is insufficient to initiate stimulated decay.

When the axion star mass exceeds the critical threshold, it collapses. As the size approaches the critical radius  $R_{\text{cr}} \simeq 24\pi\Gamma_{\phi}M_{\max}/m_{\phi}^3$  [32], stimulated decay initiates. The luminosity of the collapsing axion star from stimu-

lated decay is given by [32]

$$L_\phi = \frac{1}{2} m_\phi N_\gamma R_{cr}^{-1} = \frac{N_\gamma m_\phi^4}{48\pi\Gamma_\phi M_{\max}} \\ \sim 3.60 \times 10^{40} \text{ erg/s} \left( \frac{N_\gamma}{10^{49}} \right) \left( \frac{m_\phi}{10^{-5} \text{ eV}} \right)^2 \left( \frac{f_a}{10^{12} \text{ GeV}} \right), \quad (12)$$

where model-dependent constants  $K = 1$  and  $\kappa = 1$  are assumed. Detection of a radio signal consistent with the stimulated decay of a collapsing axion star could serve as a standard candle for constraining the Hubble constant, given the intense luminosity of such a radio burst [32].

Interestingly, radio signals from the stimulated decay of collapsing axion stars may already have been detected. FRBs are bright, transient radio emissions lasting only milliseconds [79–81], with a frequency range spanning approximately 400 MHz to 8 GHz [82] and total energy outputs typically between  $10^{38}$  and  $10^{40}$  erg [81, 83]. The photon frequency and total energy emitted by a collapsing axion star, for certain parameter ranges, align with those observed in FRBs [32]. For constraints on the axion parameter space derived from FRBs, see Ref. [32] and Fig. 1. The constraints on the axion parameter space provide valuable guidance for experimental searches for axions. The maximum axion star mass within this constrained parameter space, assuming  $\kappa = 1$ , ranges from approximately  $6.21 \times 10^{-12} M_\odot$  to  $2.61 \times 10^{-10} M_\odot$ , as shown in Fig. 1.

#### IV. ABUNDANCE OF DILUTE AXION STARS

The current relic density of axions is described by the equation [30]:

$$\Omega_\phi h^2 \simeq 0.12 \left( \frac{g_\star(T_{\text{osc}})}{106.75} \right)^{3/4} \left( \frac{m_\phi}{10^{-6} \text{ eV}} \right)^{1/2} \\ \times \left( \frac{f_a}{5.32 \times 10^{12} \text{ GeV}} \right)^2. \quad (13)$$

This equation, applicable to axions produced via the misalignment mechanism, defines the lower bound of the axion parameter space, as shown in Fig. 1. By combining Eq. (4) with Eq. (13), we obtain the axion mass  $m_\phi \simeq 1.17 \times 10^{-6}$  eV and the decay constant  $f_a \simeq 5.11 \times 10^{12}$  GeV, assuming that QCD axions constitute the majority of dark matter. Substituting these values into Eq. (6) and taking  $\kappa = 1$ , we calculate the maximum mass of the corresponding dilute axion star to be approximately  $2.61 \times 10^{-10} M_\odot$ . This value coincides with the upper limit of the maximum axion star mass, as constrained by the parameter space derived from FRBs. As shown in Fig. 1, the cosmological abundance line intersects this parameter space. This overlap significantly increases the likelihood of axions existing in this region and further supports the misalignment mechanism as a potential source of axions.

In the standard post-inflationary scenario, where  $U(1)_{\text{PQ}}$  symmetry is spontaneously broken after inflation, axion overdensities collapse during the radiation-dominated epoch, forming an early population of miniclusters with masses up to  $10^{-12} M_\odot$  [84–86]. By redshift  $z = 100$ , about 75% of axion dark matter resides within these bound structures [87], with minicluster masses reaching up to  $10^{-9} M_\odot$  due to mergers. This closely matches the mass range of  $6.21 \times 10^{-12} M_\odot$  to  $2.61 \times 10^{-10} M_\odot$  for critical axion stars constrained by FRBs. Dilute axion stars evolve toward a critical state through the accretion of axions from the surrounding environment or via merger events. Once they surpass this critical threshold, they collapse, emitting strong radio signals [31] or relativistic axions [71]. After the collapse, a residual dilute axion star remains, retaining a mass close to its critical value and entering a subcritical state. This suggests that the likelihood of dilute axion stars being in either a critical or subcritical state is relatively high. For simplicity, we will assume that dilute axion stars are in a critical state in the following discussion.

The local dark matter density  $\rho_{\text{DM}}$  near the Solar System is estimated to be  $0.01 M_\odot \text{ pc}^{-3} \approx 0.4 \text{ GeV/cm}^3$ , as inferred from stellar dynamics on scales greater than approximately 100 parsecs [88–91]. Using this value, the local number density of dilute axion stars can be calculated as:

$$n_{\text{AS}} = \frac{\Omega_{\text{AS}}}{\Omega_{\text{DM}}} \frac{\rho_{\text{DM}}}{M_{\text{AS}}} \\ = 1.27 \times 10^9 \text{ pc}^{-3} \left( \frac{\Omega_{\text{AS}}}{0.75\Omega_{\text{DM}}} \right) \left( \frac{6.21 \times 10^{-12} M_\odot}{M_{\text{AS}}} \right), \quad (14)$$

where  $\Omega_{\text{AS}}/\Omega_{\text{DM}}$  represents the fraction of dilute axion stars within dark matter. Assuming 75% of dark matter is composed of axion stars, a spherical volume with a radius of 1000 AU would contain approximately 605 axion stars with a mass of  $6.21 \times 10^{-12} M_\odot$ , or 14 axion stars with a mass of  $2.61 \times 10^{-10} M_\odot$ . The number density of dilute axion stars is inversely proportional to their mass: lower-mass axion stars are more numerous, increasing their likelihood of being present in the Solar System. This suggests that low-mass dilute axion stars, with maximum masses ranging from  $6.21 \times 10^{-12} M_\odot$  to  $2.61 \times 10^{-10} M_\odot$ , could potentially be detected within the Solar System.

#### V. ECHO FROM DILUTE AXION STARS

A dilute axion star remains stable because the photon number resulting from spontaneous decay is insufficient to initiate stimulated decay. However, by transmitting a powerful radio beam with power  $P$  to the axion star, with an angular frequency of photons equal to half the axion mass, the stimulated decay of axions can be significantly enhanced. As a result, the coupled differential equations



given by Eq. (10) and Eq. (11) are modified as follows:

$$\frac{dN_\gamma}{dt} = 2\Gamma_\phi N_\phi + \frac{12\pi}{m_\phi^3 v R_{AS}^3} \Gamma_\phi N_\phi (N_\gamma + N_{\gamma 0}) - \frac{2\pi(2v+3)}{m_\phi^3 R_{AS}^3} \Gamma_\phi (N_\gamma + N_{\gamma 0})^2 - \Gamma_e N_\gamma, \quad (15)$$

$$\frac{dN_\phi}{dt} = -\Gamma_\phi N_\phi - \frac{6\pi}{m_\phi^3 v R_{AS}^3} \Gamma_\phi N_\phi (N_\gamma + N_{\gamma 0}) + \frac{4\pi v}{m_\phi^3 R_{AS}^3} \Gamma_\phi (N_\gamma + N_{\gamma 0})^2, \quad (16)$$

where  $N_{\gamma 0} \simeq 2PR_{AS}/m_\phi$  represents the number of photons from the radio beam transmitted into the axion star. By substituting Eq. (7) into  $N_{\gamma 0}$ , we obtain

$$N_{\gamma 0} \simeq 5.02 \times 10^{28} \kappa^{1/2} \left( \frac{P}{50 \text{ MW}} \right) \times \left( \frac{m_\phi}{10^{-5} \text{ eV}} \right)^{-2} \left( \frac{f_a}{10^{12} \text{ GeV}} \right)^{-1}. \quad (17)$$

Stimulated decay dominates over spontaneous decay when the condition  $6\pi(N_\gamma + N_{\gamma 0})/(m_\phi^3 v R_{AS}^3) > 1$  is satisfied. By transmitting a powerful radio beam with a power of 50 MW into the axion star, we obtain  $N_{\gamma 0} = 3.86 \times 10^{26}$  and find that  $6\pi N_{\gamma 0}/(m_\phi^3 v R_{AS}^3) = 2.64 \times 10^{15} \gg 1$ , using the parameters  $m_\phi = 5 \times 10^{-5} \text{ eV}$ ,  $f_a = 5.20 \times 10^{12} \text{ GeV}$  and taking the model-dependent constant  $\kappa = 1$ . Thus, radio waves of sufficient power, such as  $P = 50 \text{ MW}$ , can effectively induce the stimulated decay of a dilute axion star. The multi-beam relativistic klystron amplifier currently has the capability to output radio waves with a power of 1.047 GW [92], significantly exceeding the required 50 MW. This substantial power output makes it a promising candidate for emitting radio waves to interact with axion stars. In the following discussion, we will use the example of a 50 MW radio wave received by an axion star.

Figure 2 presents two numerical solutions illustrating the evolution of the axion, photon, and “sterile” axion numbers for two representative parameter sets, assuming the model-dependent constants  $K = 1$  and  $\kappa = 1$ . The solid line represents an axion star with a critical mass of  $M_{AS} = 2.61 \times 10^{-10} M_\odot$  with parameters  $m_\phi = 1.17 \times 10^{-6} \text{ eV}$  and a decay constant  $f_a = 5.11 \times 10^{12} \text{ GeV}$ , representing the intersection of cosmological abundance and QCD axion constraints in Fig. 1. The dashed line represents an axion star with a critical mass of  $M_{AS} = 6.21 \times 10^{-12} M_\odot$ , with parameters lying within the region constrained by FRBs:  $m_\phi = 5 \times 10^{-5} \text{ eV}$  and  $f_a = 5.20 \times 10^{12} \text{ GeV}$ . For the case  $M_{AS} = 6.21 \times 10^{-12} M_\odot$ , the stimulated decay of the dilute axion star stabilizes after approximately  $10^{-4}$  seconds of irradiation, resulting in a photon number  $N_\gamma = 1.10 \times 10^{21}$ . Considering the photons escaping from the dilute axion star, the luminosity can be expressed as:

$$L_\phi = \frac{1}{2} m_\phi N_\gamma \Gamma_e. \quad (18)$$

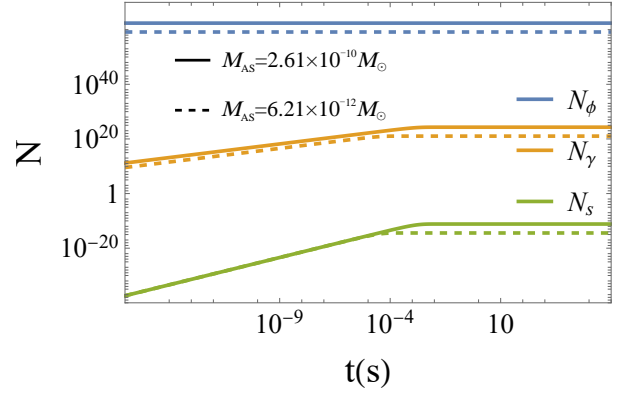


FIG. 2. Evolving axion, photon, and “sterile” axion numbers inside a dilute axion star under a 50MW radio beam. The solid line represents an axion star with a mass of  $M_{AS} = 2.61 \times 10^{-10} M_\odot$  and parameters  $m_\phi = 1.17 \times 10^{-6} \text{ eV}$  and  $f_a = 5.11 \times 10^{12} \text{ GeV}$ . The dashed line corresponds to an axion star with a mass of  $M_{AS} = 6.21 \times 10^{-12} M_\odot$  and parameters  $m_\phi = 5 \times 10^{-5} \text{ eV}$  and  $f_a = 5.20 \times 10^{12} \text{ GeV}$ . Timing begins when the axion star is irradiated with radio beam. For  $M_{AS} = 6.21 \times 10^{-12} M_\odot$ , the stimulated decay of the dilute axion star stabilizes after approximately  $10^{-4}$  seconds of irradiation, with a photon number of  $N_\gamma = 1.10 \times 10^{21}$ .

A notable feature of axion stimulated decay is that, in the axion rest frame, the emitted photons are restricted to propagate either in the same direction as or directly opposite to the incoming photons. However, within the dilute axion star, the velocity distribution of the axions leads to spatial dispersion of the emitted photons. Consequently, the luminosity flux observed from Earth is roughly given by

$$F_\phi \sim \frac{L_\phi}{4\pi d^2} = \frac{m_\phi N_\gamma \Gamma_e}{8\pi d^2}, \quad (19)$$

where  $d$  denotes the distance between the dilute axion star and Earth. For a dilute axion star in its critical state, substituting Eq. (7) into  $\Gamma_e = R_{AS}^{-1}$ , the photon escape rate becomes

$$\Gamma_e \sim 1.24 \times 10^3 \text{ s}^{-1} \kappa^{-1/2} \left( \frac{m_\phi}{10^{-5} \text{ eV}} \right) \left( \frac{f_a}{10^{12} \text{ GeV}} \right). \quad (20)$$

By substituting Eq. (20) into Eq. (19), the flux can be expressed as

$$F_\phi = 3.50 \times 10^{-35} \kappa^{-1/2} \left( \frac{m_\phi}{10^{-5} \text{ eV}} \right)^2 \left( \frac{f_a}{10^{12} \text{ GeV}} \right) \times \left( \frac{N_\gamma}{10^{20}} \right) \left( \frac{1000 \text{ AU}}{d} \right)^2 \text{ W/cm}^2. \quad (21)$$

As illustrated in Fig. 1, the critical mass of dilute axion stars constrained by FRBs ranges from approximately  $6.21 \times 10^{-12} M_\odot$  to  $2.61 \times 10^{-10} M_\odot$ . Substituting Eq.

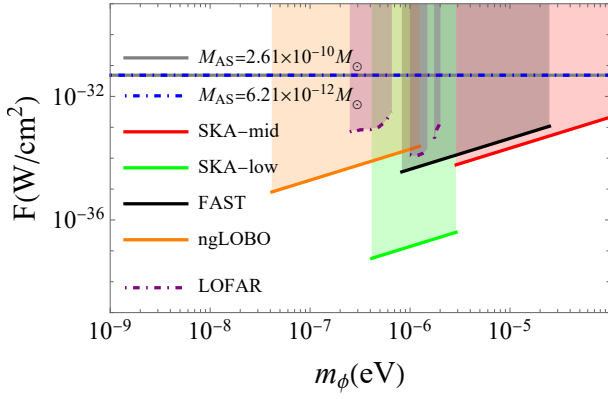


FIG. 3. Axion star flux at 1000 AU and the sensitivity of SKA, FAST, ngLOBO, and LOFAR for 1 hour observations. The sensitivity of these telescopes is detailed in Ref. [46] and its references. Even for LOFAR, the flux of the echoes is one to two orders of magnitude higher than its sensitivity, making the signal easily detectable and distinguishable.

(6) into Eq. (21) for a mass of  $6.21 \times 10^{-12} M_\odot$ , the luminosity flux of the dilute axion star is calculated as

$$F_\phi = 3.64 \times 10^{-34} \left( \frac{m_\phi}{10^{-5} \text{ eV}} \right)^3 \times \left( \frac{N_\gamma}{10^{21}} \right) \left( \frac{1000 \text{ AU}}{d} \right)^2 \text{ W/cm}^2, \quad (22)$$

corresponding to the blue dot-dashed line with a flux of  $F_\phi \approx 4.86 \times 10^{-32} \text{ W/cm}^2$  for  $d = 1000 \text{ AU}$ , as shown in Fig. 3. Similarly, substituting Eq. (6) into Eq. (21) for a mass of  $2.61 \times 10^{-10} M_\odot$  gives

$$F_\phi = 1.53 \times 10^{-32} \left( \frac{m_\phi}{10^{-6} \text{ eV}} \right)^3 \times \left( \frac{N_\gamma}{10^{24}} \right) \left( \frac{1000 \text{ AU}}{d} \right)^2 \text{ W/cm}^2, \quad (23)$$

which corresponds to the gray line for  $d = 1000 \text{ AU}$ , effectively overlapping with the blue dot-dashed line, as shown in Fig. 3. Therefore, the luminosity flux of the echo from dilute axion stars at a distance of 1000 AU, as observed from Earth, is approximately  $4.86 \times 10^{-32} \text{ W/cm}^2$ , corresponding to an axion star mass range of  $6.21 \times 10^{-12} M_\odot$  to  $2.61 \times 10^{-10} M_\odot$ , as constrained by FRBs. This flux exceeds the sensitivity thresholds of radio telescopes such as SKA, FAST, ngLOBO, and LOFAR with an observation time of 1 hour, as shown in Fig. 3. Thus, the decay signal is detectable by these radio telescopes.

Consequently, the stimulated decay of a dilute axion star within a volume of radius 1000 AU centered around Earth can be triggered by emitting a 50 MW radio beam into the star. The decay signal produces a spectral line that is almost monochromatic, with a frequency given by  $f \simeq m_\phi/(4\pi) \approx 1.21(m_\phi/10^{-5} \text{ eV}) \text{ GHz}$ , which serves as

a distinctive feature of the signal. Detection of such an echo would confirm the existence of axion stars, solve the dark matter puzzle, and provide crucial evidence linking some FRBs to axion stars. Furthermore, FRBs originating from collapsing axion stars could serve as standard candles to help resolve the Hubble tension [32]. If such echoes are not detected within a 1000 AU volume around Earth using this method, constraints can be placed on the fraction of dark matter composed of dilute axion stars with critical masses constrained by FRBs. This fraction could be roughly less than 5% for a mass of  $6.21 \times 10^{-12} M_\odot$  or 0.1% for a mass of  $2.61 \times 10^{-10} M_\odot$ , depending on the axion parameters. This estimate assumes a uniform distribution of axion stars throughout the Universe.

## VI. CONCLUSIONS

Axions are a promising candidate for dark matter. Due to their bosonic properties, they can reach exceptionally high phase space densities, which may lead to BEC and the formation of gravitationally bound objects known as axion stars. Collapsing axion stars with specific parameters may emit millisecond-long radio bursts with peak luminosities of approximately  $10^{42} \text{ erg/s}$ , which are consistent with the characteristics of observed non-repeating FRBs. If some FRBs are indeed produced by collapsing axion stars, this would impose constraints on the axion parameter space, offering valuable guidance for experimental axion searches. Thus, exploring the axion parameter space in relation to FRBs is crucial, as it relates both to the origin of FRBs and the nature of dark matter.

In the traditional post-inflationary scenario, axion stars could account for up to 75% of dark matter, suggesting that some may exist within the Solar System. Building on previous work that explored the possibility of explaining planet 9 as a dilute axion star via stimulated decay induced by a 50 MW radio beam, we propose extending this method to search for dilute axion stars with masses ranging from  $6.21 \times 10^{-12} M_\odot$  to  $2.61 \times 10^{-10} M_\odot$ . These masses are constrained by the characteristics of FRBs, which could potentially be explained by collapsing axion stars. For axions within the parameter space constrained by FRBs, the echo resulting from the stimulated decay of axion stars could be detectable by ground-based radio telescopes. Detection of such an echo would not only confirm the existence of axion stars but also provide key evidence linking axion stars to FRBs. Furthermore, using FRBs from axion star collapses as standard candles could aid in resolving the Hubble tension. If no signal is detected, this method will provide constraints on the abundance of dark matter in the form of dilute axion stars with masses between  $6.21 \times 10^{-12} M_\odot$  and  $2.61 \times 10^{-10} M_\odot$ . Under the assumption of a uniform distribution of dilute axion stars across the Universe, the abundance would be limited to less than approximately 5% for masses of  $6.21 \times 10^{-12} M_\odot$  or 0.1% for masses of  $2.61 \times 10^{-10} M_\odot$ .

## ACKNOWLEDGMENTS

H. D. would like to thank Lijing Shao for useful discussions. This work was supported by National Nat-

ural Science Foundation of China under Grant No. 11947031 and East China University of Technology Research Foundation for Advanced Talents under Grant No. DHBK2019206.

- 
- [1] S. Weinberg, A new light boson?, *Phys. Rev. Lett.* **40**, 223 (1978).
  - [2] F. Wilczek, Problem of strong  $P$  and  $T$  invariance in the presence of instantons, *Phys. Rev. Lett.* **40**, 279 (1978).
  - [3] R. D. Peccei and H. R. Quinn, Constraints imposed by CP conservation in the presence of pseudoparticles, *Phys. Rev. D* **16**, 1791 (1977).
  - [4] R. D. Peccei and H. R. Quinn, CP conservation in the presence of pseudoparticles, *Phys. Rev. Lett.* **38**, 1440 (1977).
  - [5] A. Arvanitaki, S. Dimopoulos, S. Dubovsky, N. Kaloper and J. March-Russell, String axiverse, *Phys. Rev. D* **81**, 123530 (2010).
  - [6] J. Preskill, M. B. Wise and F. Wilczek, Cosmology of the invisible axion, *Phys. Lett. B* **120**, 127 (1983).
  - [7] L. F. Abbott and P. Sikivie, A cosmological Bbound on the invisible axion, *Phys. Lett. B* **120**, 133 (1983).
  - [8] M. Dine and W. Fischler, The not so harmless axion, *Phys. Lett. B* **120**, 137 (1983).
  - [9] R. T. Co, L. J. Hall and K. Harigaya, Axion kinetic misalignment mechanism, *Phys. Rev. Lett.* **124**, 251802 (2020).
  - [10] M. S. Turner, Early-universe thermal production of not-so-invisible axions, *Phys. Rev. Lett.* **59**, 2489 (1987); Erratum, *Phys. Rev. Lett.* **60**, 1101 (1988).
  - [11] A. Salvio, A. Strumia and W. Xue, Thermal axion production, *JCAP* **01**, 011 (2014).
  - [12] R. L. Davis, Cosmic axions from cosmic strings, *Phys. Lett. B* **180**, 225 (1986).
  - [13] M. Gorghetto, E. Hardy and G. Villadoro, More axions from strings, *SciPost Phys.* **10**, 050 (2021).
  - [14] F. Schiavone, D. Montanino, A. Mirizzi and F. Capozzi, Axion-like particles from primordial black holes shining through the Universe, *JCAP* **08**, 063 (2021).
  - [15] T. Li and R. J. Zhang, Axionlike particles from primordial black hole evaporation and their detection in neutrino experiments, *Phys. Rev. D* **106**, 095034 (2022).
  - [16] K. Mazde and L. Visinelli, The interplay between the dark matter axion and primordial black holes, *JCAP* **01**, 021 (2023).
  - [17] P. Sikivie and Q. Yang, Bose-Einstein condensation of dark matter axions, *Phys. Rev. Lett.* **103**, 111301 (2009).
  - [18] E. Braaten and H. Zhang, Colloquium : The physics of axion stars, *Rev. Mod. Phys.* **91**, 041002 (2019).
  - [19] L. Visinelli, Boson stars and oscillatons: A review, *Int. J. Mod. Phys. D* **30**, 2130006 (2021).
  - [20] M. Gorghetto, E. Hardy and G. Villadoro, More axion stars from strings, *JHEP* **08**, 126 (2024).
  - [21] J. H. Chang, P. J. Fox and H. Xiao, Axion stars: mass functions and constraints, *JCAP* **08**, 023 (2024).
  - [22] H. Y. Zhang, Unified view of scalar and vector dark matter solitons, [arXiv:2406.05031](https://arxiv.org/abs/2406.05031).
  - [23] M. E. Brown, C. Trujillo and D. Rabinowitz, Discovery of a candidate inner Oort cloud planetoid, *Astrophys. J.* **617**, 645 (2004).
  - [24] C. Trujillo, and S. S. Sheppard, A Sedna-like body with a perihelion of 80 astronomical units, *Nature* **507**, 471 (2014).
  - [25] K. Batygin and M. E. Brown, Evidence for a distant giant planet in the Solar System, *Astron. J.* **151**, 22 (2016).
  - [26] P. Mroz, A. Udalski, J. Skowron, R. Poleski, S. Kozłowski, M. K. Szymanski, I. Soszynski, L. Wyrzykowski, P. Pietrukowicz, K. Ulaczyk *et al.*, No large population of unbound or wide-orbit Jupiter-mass planets, *Nature* **548**, 183 (2017).
  - [27] H. Niikura, M. Takada, S. Yokoyama, T. Sumi and S. Masaki, Constraints on Earth-mass primordial black holes from OGLE 5-year microlensing events, *Phys. Rev. D* **99**, 083503 (2019).
  - [28] S. Sugiyama, M. Takada and A. Kusenko, Possible evidence of axion stars in HSC and OGLE microlensing events, *Phys. Lett. B* **840**, 137891 (2023).
  - [29] K. Batygin, F. C. Adams, M. E. Brown, J. C. Becker, The planet nine hypothesis, *Phys. Rep.* **805**, 1 (2019).
  - [30] H. Di and H. Shi, Can planet 9 be an axion star?, *Phys. Rev. D* **108**, 103038 (2023).
  - [31] H. Di, Stimulated decay of collapsing axion stars and fast radio bursts, *Eur. Phys. J. C* **84**, 283 (2024).
  - [32] H. Di, L. Shao, Z. Yi and S. B. Kong, Novel standard candle: Collapsing axion stars, *Phys. Rev. D* **110**, 103031 (2024).
  - [33] A. Iwazaki, Axion stars and fast radio bursts, *Phys. Rev. D* **91**, 023008 (2015).
  - [34] I. I. Tkachev, Fast radio bursts and axion miniclusters, *JETP Lett.* **101**, 1 (2015).
  - [35] S. Raby, Axion star collisions with neutron stars and fast radio bursts, *Phys. Rev. D* **94**, 103004 (2016).
  - [36] J. H. Buckley, P. S. B. Dev, F. Ferrer and F. P. Huang, Fast radio bursts from axion stars moving through pulsar magnetospheres, *Phys. Rev. D* **103**, 043015 (2021).
  - [37] T. W. Kephart and T. J. Weiler, Stimulated radiation from axion cluster evolution, *Phys. Rev. D* **52**, 3226 (1995).
  - [38] J. G. Rosa and T. W. Kephart, Stimulated axion decay in superradiant clouds around primordial black holes, *Phys. Rev. Lett.* **120**, 231102 (2018).
  - [39] A. Caputo, M. Regis, M. Taoso and S. J. Witte, Detecting the stimulated decay of axions at radio frequencies, *JCAP* **03**, 027 (2019).
  - [40] P. S. B. Dev, F. Ferrer and T. Okawa, On the Galactic radio signal from stimulated decay of axion dark matter, *JCAP* **04**, 045 (2024).
  - [41] A. Arza and P. Sikivie, Production and detection of an axion dark matter echo, *Phys. Rev. Lett.* **123**, 131804 (2019).
  - [42] A. Arza and E. Todarello, Axion dark matter echo: A detailed analysis, *Phys. Rev. D* **105**, 023023 (2022).
  - [43] A. Arza, A. Kryemadhi and K. Zioutas, Searching for axion streams with the echo method, *Phys. Rev. D* **108**, 083001 (2023).

- [44] A. Arza, Q. Guo, L. Wu, Q. Yang, X. Yang, Q. Yuan and B. Zhu, Listening for echo from the stimulated axion decay with the 21 centimeter array, *Sci. Bull.* **69**, 2971 (2024).
- [45] Y. Gong, X. Liu, L. Wu, Q. Yang and B. Zhu, Detecting quadratically coupled ultralight dark matter with stimulated annihilation, *Phys. Rev. D* **109**, 055026 (2024).
- [46] H. Di, H. Shi and Z. Yi, Detection of dilute axion stars with stimulated decay, *Phys. Rev. D* **111**, 023011 (2025).
- [47] J. Scholtz and J. Unwin, What if planet 9 is a primordial black hole?, *Phys. Rev. Lett.* **125**, 051103 (2020).
- [48] P. Di Vecchia and G. Veneziano, Chiral dynamics in the large  $n$  limit, *Nucl. Phys. B* **171**, 253 (1980).
- [49] G. Grilli di Cortona, E. Hardy, J. Pardo Vega and G. Villadoro, The QCD axion, precisely, *JHEP* **01**, 034 (2016).
- [50] K. Fujikura, M. P. Hertzberg, E. D. Schiappacasse and M. Yamaguchi, Microlensing constraints on axion stars including finite lens and source size effects, *Phys. Rev. D* **104**, 123012 (2021).
- [51] E. D. Schiappacasse and M. P. Hertzberg, Analysis of dark matter axion clumps with spherical symmetry, *JCAP* **01**, 037 (2018); Erratum, *JCAP* **03**, E01 (2018).
- [52] P. H. Chavanis, Phase transitions between dilute and dense axion stars, *Phys. Rev. D* **98**, 023009 (2018).
- [53] L. Visinelli, S. Baum, J. Redondo, K. Freese and F. Wilczek, Dilute and dense axion stars, *Phys. Lett. B* **777**, 64 (2018).
- [54] J. Eby, M. Leembruggen, L. Street, P. Suranyi and L. C. R. Wijewardhana, Global view of QCD axion stars, *Phys. Rev. D* **100**, 063002 (2019).
- [55] E. Seidel and W. M. Suen, Oscillating soliton stars, *Phys. Rev. Lett.* **66**, 1659 (1991).
- [56] M. P. Hertzberg, Quantum radiation of oscillons, *Phys. Rev. D* **82**, 045022 (2010).
- [57] J. Eby, P. Suranyi and L. C. R. Wijewardhana, The lifetime of axion stars, *Mod. Phys. Lett. A* **31**, 1650090 (2016).
- [58] Z. Wang, L. Shao and L. X. Li, Resonant instability of axionic dark matter clumps, *JCAP* **07**, 038 (2020).
- [59] P. H. Chavanis, Mass-radius relation of Newtonian self-gravitating Bose-Einstein condensates with short-range interactions: I. Analytical results, *Phys. Rev. D* **84**, 043531 (2011).
- [60] P. H. Chavanis and L. Delfini, Mass-radius relation of Newtonian self-gravitating Bose-Einstein condensates with short-range interactions: II. Numerical results, *Phys. Rev. D* **84**, 043532 (2011).
- [61] B. C. Mundim, A numerical study of boson star binaries, *arXiv:1003.0239*.
- [62] E. Cotner, Collisional interactions between self-interacting nonrelativistic boson stars: Effective potential analysis and numerical simulations, *Phys. Rev. D* **94**, 063503 (2016).
- [63] B. Schwabe, J. C. Niemeyer and J. F. Engels, Simulations of solitonic core mergers in ultralight axion dark matter cosmologies, *Phys. Rev. D* **94**, 043513 (2016).
- [64] J. Eby, M. Leembruggen, J. Leeney, P. Suranyi and L. C. R. Wijewardhana, Collisions of dark matter axion stars with astrophysical sources, *JHEP* **04**, 099 (2017).
- [65] M. P. Hertzberg, Y. Li and E. D. Schiappacasse, Merger of dark matter axion clumps and resonant photon emission, *JCAP* **07**, 067 (2020).
- [66] X. Du, D. J. E. Marsh, M. Escudero, A. Benson, D. Blas, C. K. Pooni and M. Fairbairn, Soliton merger rates and enhanced axion dark matter decay, *Phys. Rev. D* **109**, 043019 (2024).
- [67] D. Maseizik and G. Sigl, Distributions and collision rates of ALP stars in the Milky Way, *Phys. Rev. D* **110**, 083015 (2024).
- [68] J. Chen, X. Du, E. W. Lentz, D. J. E. Marsh and J. C. Niemeyer, New insights into the formation and growth of boson stars in dark matter halos, *Phys. Rev. D* **104**, 083022 (2021).
- [69] J. H. H. Chan, S. Sibiryakov and W. Xue, Condensation and evaporation of boson stars, *JHEP* **01**, 071 (2024).
- [70] A. S. Dmitriev, D. G. Levkov, A. G. Panin and I. I. Tkachev, Self-similar growth of bose stars, *Phys. Rev. Lett.* **132**, 091001 (2024).
- [71] D. G. Levkov, A. G. Panin and I. I. Tkachev, Relativistic axions from collapsing Bose stars, *Phys. Rev. Lett.* **118**, 011301 (2017).
- [72] P. H. Chavanis, Collapse of a self-gravitating Bose-Einstein condensate with attractive self-interaction, *Phys. Rev. D* **94**, 083007 (2016).
- [73] J. Eby, M. Leembruggen, P. Suranyi and L. C. R. Wijewardhana, Collapse of axion stars, *JHEP* **12**, 066 (2016).
- [74] P. J. Fox, N. Weiner and H. Xiao, Recurrent axion stars collapse with dark radiation emission and their cosmological constraints, *Phys. Rev. D* **108**, 095043 (2023).
- [75] L. Caloni, M. Gerbino, M. Lattanzi and L. Visinelli, Novel cosmological bounds on thermally-produced axion-like particles, *JCAP* **09**, 021 (2022).
- [76] K. Springmann, M. Stadlbauer, S. Stelzl and A. Weiler, A universal bound on QCD axions from supernovae, *arXiv:2410.19902*.
- [77] R. Balkin, J. Serra, K. Springmann, S. Stelzl and A. Weiler, White dwarfs as a probe of exceptionally light QCD axions, *Phys. Rev. D* **109**, 095032 (2024).
- [78] A. Gómez-Bañón, K. Bartnick, K. Springmann and J. A. Pons, Constraining light QCD axions with isolated neutron star cooling, *Phys. Rev. Lett.* **133**, 251002 (2024).
- [79] D. R. Lorimer, M. Bailes, M. A. McLaughlin, D. J. Narkevic, and F. Crawford, A bright millisecond radio burst of extragalactic origin, *Science*, **318**, 777 (2007).
- [80] E. F. Keane, B. W. Stappers, M. Kramer and A. G. Lyne, On the origin of a highly-dispersed coherent radio burst, *Mon. Not. Roy. Astron. Soc.* **425**, 71 (2012).
- [81] D. Thornton, B. Stappers, M. Bailes, B. R. Barsdell, S. D. Bates, N. D. R. Bhat, M. Burgay, S. Burke-Spolaor, D. J. Champion, P. Coster *et al.*, A population of fast radio bursts at cosmological distances, *Science* **341**, 53 (2013).
- [82] E. Petroff, J. W. T. Hessels and D. R. Lorimer, Fast radio bursts, *Astron. Astrophys. Rev.* **27**, 4 (2019).
- [83] L. G. Spitler, J. M. Cordes, J. W. T. Hessels, D. R. Lorimer, M. A. McLaughlin, S. Chatterjee, F. Crawford, J. S. Deneva, V. M. Kaspi, R. S. Wharton *et al.*, Fast radio burst discovered in the arecibo pulsar ALFA survey, *Astrophys. J.* **790**, 101 (2014).
- [84] C. J. Hogan and M. J. Rees, Axion miniclusters, *Phys. Lett. B* **205**, 228 (1988).
- [85] E. W. Kolb and I. I. Tkachev, Axion miniclusters and bose stars, *Phys. Rev. Lett.* **71**, 3051 (1993).
- [86] E. W. Kolb and I. I. Tkachev, Femtolensing and picolensing by axion miniclusters, *Astrophys. J. Lett.* **460**, L25 (1996).
- [87] B. Eggemeier, J. Redondo, K. Dolag, J. C. Niemeyer and



- A. Vaquero, First simulations of axion minicluster halos, [Phys. Rev. Lett. \*\*125\*\*, 041301 \(2020\)](#).
- [88] J. I. Read, The local dark matter density, [J. Phys. G \*\*41\*\*, 063101 \(2014\)](#).
- [89] P. J. McMillan, The mass distribution and gravitational potential of the Milky Way, [Mon. Not. Roy. Astron. Soc. \*\*465\*\*, 76 \(2016\)](#).
- [90] N. W. Evans, C. A. J. O'Hare and C. McCabe, Refinement of the standard halo model for dark matter searches in light of the Gaia Sausage, [Phys. Rev. D \*\*99\*\*, 023012 \(2019\)](#).
- [91] P. F. de Salas and A. Widmark, Dark matter local density determination: recent observations and future prospects, [Rept. Prog. Phys. \*\*84\*\*, 104901 \(2021\)](#).
- [92] L. Sun et al., Compact, stable, repetitive GW-level S-band multibeam relativistic klystron amplifier operating over a longer period in a lower magnetic field, [IEEE Trans. Electron Devices \*\*70\*\*, 6571 \(2023\)](#).